

Germanium on double-SOI photodetectors for 1550 nm operation

O. I. Dosunmu^a, D. D. Cannon^b, M. K. Emsley^a, B. Ghyselen^c, J. Liu^b, L. C. Kimerling^b,
and M. S. Ünlü^a

^aBoston University, Department of Electrical and Computer Engineering, 8 Saint Mary's Street,
Boston, MA 02215;

^bDepartment of Materials Science and Engineering, Massachusetts Institute of Technology,
Cambridge, MA 02139;

^cSOITEC SA, Parc Technologique des Fontaines, 38190 Bernin, France

ABSTRACT

We have fabricated and characterized the first resonant cavity enhanced (RCE) germanium photodetectors on double silicon-on-insulator substrates (Ge/DSOI) for operation around the 1550 nm communication wavelength. The Ge layer is grown through a novel two-step UHV/CVD process, while the underlying double-SOI substrate is formed through an ion-cut process. Absorption measurements of an undoped Ge-on-Si (Ge/Si) structure reveal a red-shift of the Ge absorption edge in the NIR, due primarily to a strain-induced bandgap narrowing within the Ge film. By using the strained-Ge absorption coefficients extracted from the absorption measurements, in conjunction with the known properties of the DSOI substrate, we were able to design strained-Ge/DSOI photodetectors optimized for 1550 nm operation. We predict a quantum efficiency of 76% at 1550 nm for a Ge layer thickness of only 860 nm as a result of both strain-induced and resonant cavity enhancement, compared to 2.3% for the same unstrained Ge thickness in a single-pass configuration. We also estimate a transit-time limited bandwidth of 28 GHz. Although the fabricated Ge/DSOI photodetectors were not optimized for 1550 nm operation, we were able to demonstrate an over four-fold improvement in the quantum efficiency, compared to its single-pass counterpart.

Keywords: Photodetector, germanium, SOI, bandgap narrowing, resonant cavity

1. INTRODUCTION

The widespread demand for high speed data communications is driving the optical communications industry into devising more cost-effective ways of meeting these demands. Presently, full integration of photonic elements into the silicon-based electronics of the optical communications infrastructure has become one of the major focuses of this industry. As a result, silicon-based optoelectronics, photodetectors in particular, have received widespread attention. Although major strides have been made in designing Si-based photodetectors for short-haul (850 nm) operation,^{1,2} long-haul operation based around the 1.3 – 1.55 μm wavelength range still poses a great challenge. The complete transparency of silicon at wavelengths beyond 1.1 μm makes it unsuited for photodetection around the 1.3 – 1.55 μm wavelength range. The integration of other semiconductors with silicon, InGaAs for example (see Fig. 1), which are better suited for photodetection at these wavelengths has also been extensively explored, most notably through the methods of flip-chip bonding as well as through heteroepitaxial growth directly onto silicon. The silicon optical bench (SiOB) technology, for example, has been successful in combining the high performance of silicon electronics with the appealing optical properties of III-V semiconductors through a flip-chip hybrid integration technique.^{3,4} However, the inherent complexity of the required lift-off and micro-self-alignment process characteristic of this technique, especially on a large scale, makes it quite costly.⁵ As for the heteroepitaxial growth of a compound semiconductor such as InGaAs directly onto Si, the large lattice mismatch which exists between InGaAs and Si (> 9%) would make the growth of uniform high quality InGaAs films extremely difficult, if not impossible. In addition, attempting to grow a compound semiconductor onto an elemental material such as Si often results in the formation of anti-phase domains, further degrading the quality of the film being grown. It is for this very reason that elemental semiconductors are better suited for heteroepitaxial growth onto Si.

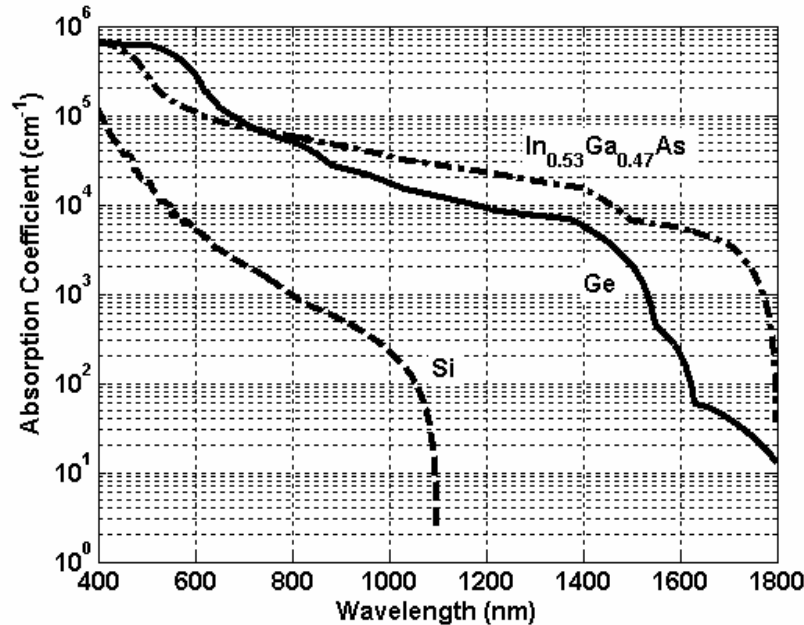


Figure 1: Absorption coefficients for various semiconductors

2. MOTIVATION AND DESIGN

Germanium is a viable candidate for integration on Si, given its sensitivity at the 1.3 – 1.55 μm communication wavelengths due to its smaller indirect bandgap of 0.64 eV, as well as its compatibility with integrated circuit technologies. In addition, unlike InGaAs, Ge is an elemental semiconductor. However, the relatively weak absorption ($\sim 460 \text{ cm}^{-1}$) of Ge at 1550 nm would necessitate a thick active region in order to achieve high efficiency, resulting in a very slow device. In a vertical single-pass configuration, for example, a 22 μm thick Ge film would be required to obtain a QE of 40% at 1550 nm, resulting in a carrier transit time of approximately 1.2 ns. One way to effectively enhance the response of a weakly absorbing medium, without sacrificing the device bandwidth, involves placing the absorbing medium within a Fabry-Perot, or resonant, cavity.⁶ In a resonant cavity enhanced (RCE) configuration, a multiple-pass photodetection scheme is created, which effectively reduces the absorbing region thickness required to obtain a given QE at a particular wavelength, in turn enhancing the device bandwidth. For example, an RCE Si-based vertical PIN photodetector has been recently demonstrated,² where a 2 μm thick Si active region is epitaxially grown on a distributed Bragg reflector (DBR) consisting of two periods of Si/SiO₂, or double-SOI (DSOI), optimized for high reflectivity over a broad range of wavelengths centered at 850 nm. At 850 nm, this photodetector exhibited a QE of 40%, with a 3dB bandwidth in excess of 10 GHz.

Applying this RCE technique to Ge in order to enhance its effective absorption at 1550 nm will first require a DBR structure optimized for high reflectivity around 1550 nm. Figure 2 illustrates the simulated and measured reflectivity of a DSOI structure we have designed to be highly reflective in the 1300 – 1550 nm wavelength range.⁷ This DSOI substrate is fabricated through an ion-cut process,^{8,9} where the basic mechanism is based on the blistering of Si. The blistering process occurs when a Si substrate implanted with a high dose of hydrogen ions is heated. The gas pressure in the Si causes microcavities which are formed close to the hydrogen implant depth range, resulting in the formation and propagation of fractures which cause the surface to blister and peel. The transfer of thin Si layers can be realized by bonding a hydrogen-implanted substrate to another Si handle wafer prior to blistering. To create an SOI wafer, the wafer to be blistered is oxidized before hydrogen implantation. The blistering process results in a rough Si surface, which can be smoothed through chemomechanical polishing. Through this process, a wide range of Si and SiO₂ thicknesses are possible. In addition, because the implanted hydrogen ions are relatively light, no detectable crystalline damage to the SOI is caused. In fabricating a double-SOI (DSOI) substrate, the ion-cut process is merely repeated. That is, the hydrogen-implanted oxidized Si wafer is bonded to another SOI wafer instead of a Si

handle wafer. For our DSOI wafer optimized for high reflectivity around 1550 nm, the thicknesses of the Si and SiO₂ layers are 300 nm and 250 nm, respectively. Requiring only two periods of Si/SiO₂ because of the high index contrast between the Si and SiO₂ layers (at 1550 nm, $n_{Si}/n_{SiO_2} \approx 2.4$), the DSOI structure is designed to provide greater than 90% free-space reflectivity over a 325 nm spectral range centered around 1400 nm, with 92.7% reflectivity at 1550 nm.

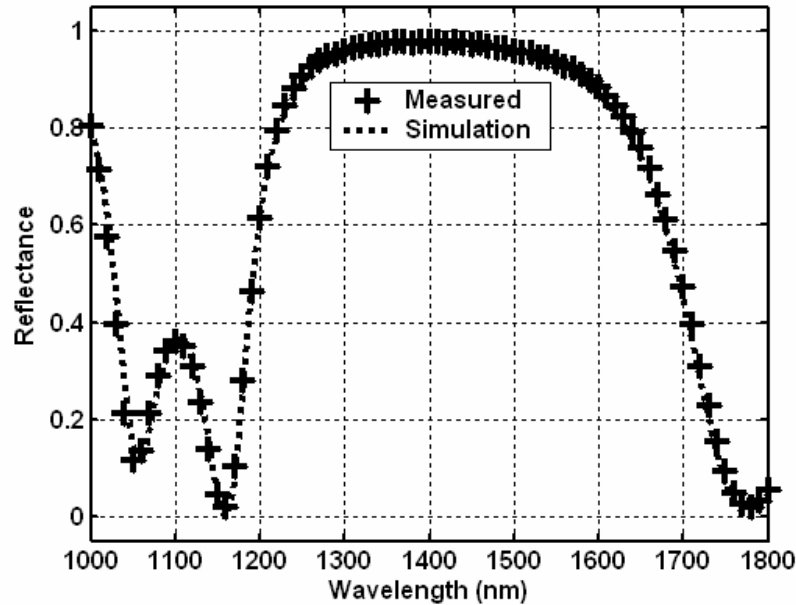


Figure 2: Simulated and measured reflectivity of the DSOI structure in the NIR

Given a Ge layer grown on a DSOI optimized for high reflectivity around 1550 nm, one can design a structure that can provide a responsivity at 1550 nm many times greater than that obtainable in a single-pass configuration, using a much thinner Ge film. However, the growth of high quality Ge films on Si can prove to be challenging. The difficulty in Ge heteroepitaxy onto Si stems from the 3.96% lattice mismatch between Ge and Si. The misfit and threading dislocations resulting from such a lattice mismatch severely limits the thickness of high quality Ge films obtainable while introducing large leakage currents, reducing the overall photodetector response attainable. Recently, a two-step ultrahigh vacuum/chemical vapor deposition (UHV/CVD) direct epitaxial growth process has been developed for Ge growth onto Si, along with a cyclic annealing process which dramatically reduces the threading dislocation density within the heteroepitaxially grown Ge film.¹⁰ In this process, a thin low temperature Ge buffer layer is grown at a temperature of 375°C to a thickness of about 30 nm. Afterwards, the growth temperature is increased to around 600°C, and the growth of a thick, uniform Ge film is performed.

In designing an RCE Ge/DSOI photodetector for operation at 1550 nm, the Ge layer thickness must be chosen not only to be resonant at 1550 nm, but also to optimize the detector bandwidth. However, before the optimum Ge thickness can be determined, the absorptive properties of the Ge film have to be known. The absorption characteristics of an undoped Ge/Si test sample were measured, where the Ge layer was grown through the aforementioned two-step UHV/CVD process, and an enhancement in absorption was observed with respect to bulk Ge. This extra enhancement is attributed to the tensile strain-induced bandgap narrowing within the Ge layer, resulting from the difference in the thermal expansion coefficients of Ge and Si.¹¹ Although the Ge layer is relaxed during growth, strain is introduced as the structure is cooled to room temperature. Because this strain-induced enhancement is a bulk effect,¹¹ the enhanced effective absorption coefficients of the strained Ge layer can be extracted from the absorption data. Illustrated in Fig. 3 are the absorption coefficients of the strained Ge layer above 1300 nm, extracted from the measured absorption of the undoped Ge/Si wafer sample, which show about an order of magnitude increase at 1550 nm with respect to the bulk Ge values.¹² X-Ray diffraction measurements reveal a Ge film strain of 0.221% for the Ge/DSOI structure, as opposed to 0.2% strain reported for its Ge/Si counterpart.¹¹ This translates to an absorption edge red-shift of

approximately 5 nm for the Ge/DSOI structure, compared to Ge/Si, with virtually no change in the enhanced absorption coefficient at 1550 nm. Therefore, the response of a Ge/DSOI structure optimized for 1550 nm operation can be simulated using the Ge absorption coefficients extracted from the Ge/Si structure.

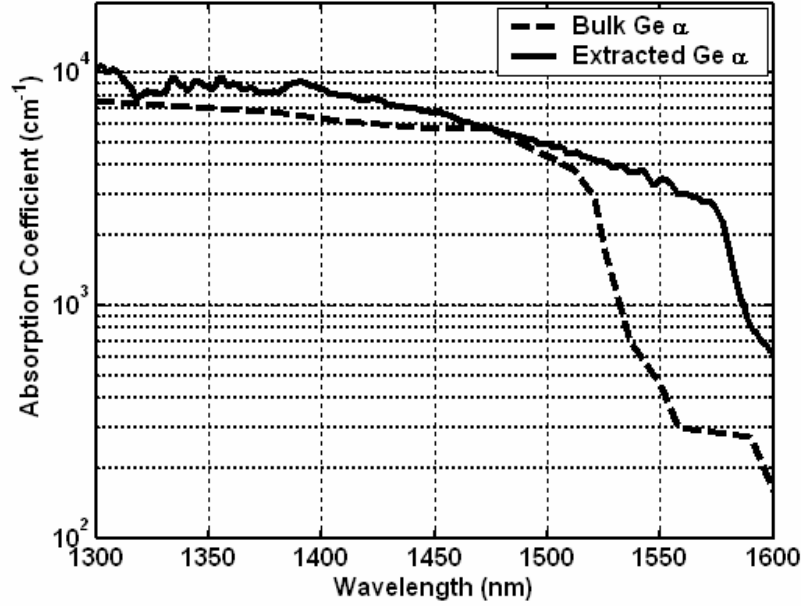


Figure 3: A comparison of the extracted strained-Ge absorption coefficients to bulk-Ge values. Extracted values were from an undoped Ge/Si sample, and bulk-Ge values were obtained from Ref. 12.

The quantum efficiency of an RCE photodetector is given by the following expression:⁶

$$\eta = \left\{ \frac{(1 + R_2 e^{-\alpha L})}{1 - 2\sqrt{R_1 R_2} e^{-\alpha L} \cos(2\beta L + \psi_1 + \psi_2) + R_1 R_2 e^{-2\alpha L}} \right\} \times (1 - R_1)(1 - e^{-\alpha L}), \quad (1)$$

where α and L represent the absorption coefficient and thickness of the active region, respectively. Other variables represented in this expression are the top (R_1) and bottom (R_2) cavity mirror reflectivity, the top (ψ_1) and bottom (ψ_2) mirror phase shifts, and the propagation constant $\beta = 2\pi n/\lambda_0$, where λ_0 represents the free-space wavelength. For the same RCE photodetector, the 3dB bandwidth can be approximated by the following expression:

$$f_{3dB} = \left(\frac{1}{f_{tr}} + \frac{1}{f_{RC}} \right)^{-1} = \left[\frac{L}{0.45v} + \frac{2\pi R \epsilon A}{L} \right]^{-1}, \quad (2)$$

where f_{tr} and f_{RC} represent the transit-time and capacitance-limited bandwidths, respectively. Also represented in this expression are the charge carrier velocity v , detector area A , and resistance R . Given these two expressions, and assuming a small area ($< 30 \mu\text{m}$ diameter) Ge/DSOI device, an optimum strained-Ge layer thickness of 860 nm is calculated for 1550 nm operation. As is illustrated in Fig. 4, given a Ge layer thickness of only 860 nm, a quantum efficiency of 76% at 1550 nm is attainable, assuming that all the absorbed photons contribute to the measured photocurrent. This simulated QE value is almost five times that obtainable with a strained-Ge/Si structure, and 33 times the QE of an unstrained-Ge/Si structure at 1550 nm, assuming equivalent Ge layer thicknesses. In terms of the device bandwidth, a Ge layer thickness of 860 nm would result in a transit-time limited bandwidth of 28.3 GHz, making such a photodetector compatible with 10 Gb/s data communication systems.

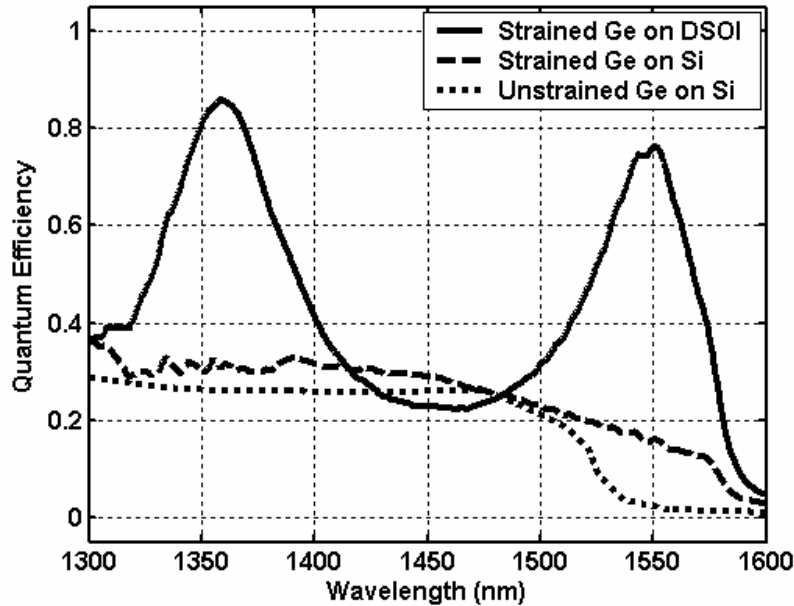


Figure 4: QE simulation of the Ge/DSOI photodetector optimized for 1550 nm operation, compared to both strained and unstrained Ge/Si; Ge thickness: 860 nm. Simulations assume 100% carrier collection.

3. RESULTS AND DISCUSSIONS

We have fabricated the first resonant cavity enhanced Ge on DSOI photodetectors for operation around 1550 nm. As can be seen in the cross-sectional view in Fig. 5, our photodetector is a top-illuminated PIN structure, which consists of a Ge layer grown via the two-step UHV/CVD process onto the DSOI substrate described earlier, although it is important to note that this structure was not cyclic annealed. The contact regions are defined through the ion-implantation of phosphorus in the Ge film, and boron in the top Si layer. Photodetector mesas of various sizes ranging from $140\ \mu\text{m} \times 140\ \mu\text{m}$ to $1\ \text{mm} \times 1\ \text{mm}$ were etched, and silver metal pads were patterned to contact the ion-implanted *P* and *N* regions of the photodetector structure.

Figure 6 compares the response of one of our fabricated Ge/DSOI photodetectors at room temperature to its simulated response. Here, both the simulated and measured quantum efficiencies of this detector are lower at 1550 nm than that anticipated for the optimized detector simply because the 755 nm thick Ge layer is not resonant at 1550 nm. The resonant response of an RCE detector can be adjusted through recess etching, although care must be taken not to etch away the top contact region. To improve the response of this particular photodetector, the Ge layer was etched back to a thickness of 737 nm and a 300 nm SiO_2 layer was sputtered onto the detection area. At 1550 nm, the photodetector was measured having a 14% quantum efficiency at 2 V reverse bias, which is over four times the simulated QE of 3.33% in a single pass configuration without strain-induced absorption enhancement. However, this measured response is less than half the expected QE of 33.3%. The most likely reason for the discrepancy between the expected and measured QE stems from the photogenerated carriers not being collected efficiently at the contacts. One contributing factor to the loss of photogenerated carriers is carrier recombination at the threading dislocation sites within the Ge layer. To reduce recombination at these defect sites, the photodetector is reverse biased, increasing the photogenerated carrier velocities and reducing the carrier interaction time with the threading dislocation sites. This is evident when compared to the photodetector response at zero bias as seen in Fig. 5, which falls to about 8.6% at 1550 nm.

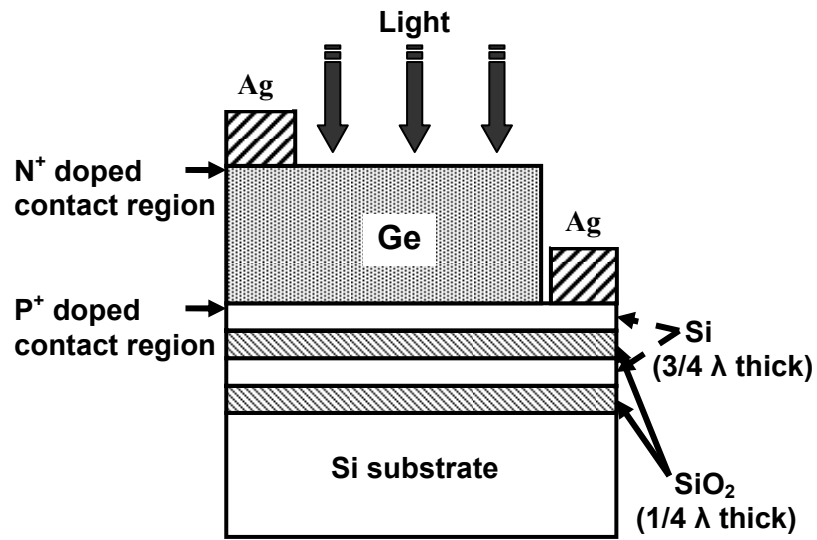


Figure 5: Cross-sectional view of the top-illuminated Ge/DSOI vertical PIN photodetector; Ge thickness: 755 nm.

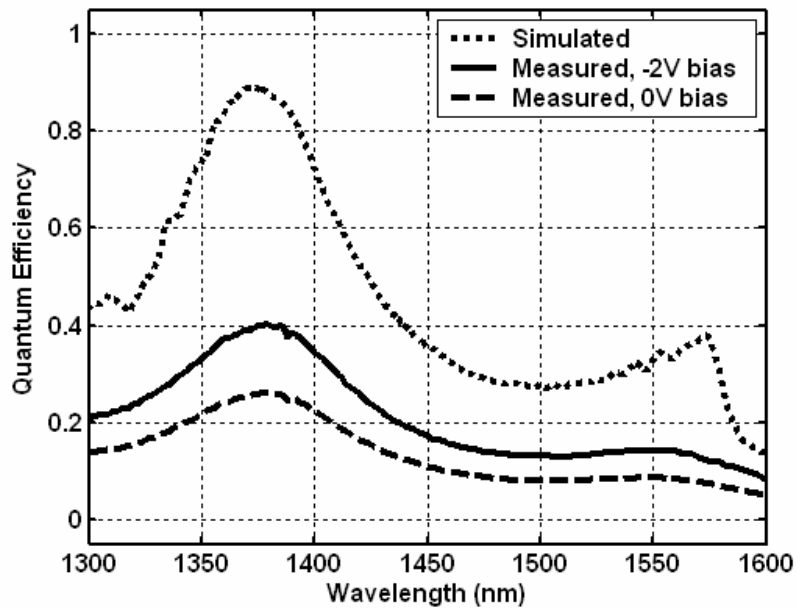


Figure 6: Measured Ge/DSOI photodetector QE at 0V and 2V reverse bias vs. simulated QE. The 140 μm by 140 μm area device includes a 737 nm Ge layer, capped with a 300 nm SiO₂ layer. Simulation assumes 100% carrier collection.

4. CONCLUSIONS

We have simulated and fabricated Ge/DSOI photodetectors which are suitable for operation at 1550 nm. When optimized, our detectors should exhibit quantum efficiencies of nearly 80% at 1550 nm, with a transit-time limited bandwidth approaching 30GHz. The enhanced response of these detectors is attributed to both the resonant cavity effect as well as the strain-induced bandgap narrowing within the Ge layer. Although our fabricated Ge/DSOI detector was not optimized for 1550 nm operation, it still exhibited over a four-fold QE improvement compared to its unstrained single-pass counterpart.

ACKNOWLEDGEMENTS

The authors would like to thank Mike Ameen and Mark Harris at Axcelis Technologies for their implantation efforts. Parts of the fabrication process were performed at the Microsystems Technology Laboratory at MIT.

This research was sponsored by the Army Research Laboratory (ARL) and was accomplished under the ARL Cooperative Agreement Number DAAD17-99-2-0070. The views and conclusions contained in this document are those of the authors and should not be interpreted as representing the Laboratory or the U.S. Government. The U.S. Government is authorized to reproduce and distribute reprints for Government purposes notwithstanding any copyright notation hereon.

REFERENCES

- ¹ J.D. Schuab, R. Li, C.L. Schow, and J.C. Campbell, "Resonant-Cavity-Enhanced High-Speed Si Photodiode Grown by Epitaxial Lateral Overgrowth," *IEEE Phot. Tech. Lett.*, **Vol. 11** (12), 1647–1649, 1999.
- ² M. K. Emsley, O. I. Dosunmu, and M. S. Ünlü, "High-Speed Resonant-Cavity-Enhanced Silicon Photodetectors on Reflecting Silicon-on-Insulator Substrates," *IEEE Photon. Tech. Lett.*, **Vol. 14** (4), 519–521, 2002.
- ³ A. V. Krishnamoorthy and D. A. B. Miller, "Scaling optoelectronic-VLSI circuits into the 21st century: A technology roadmap," *IEEE J. Select. Top. Quantum Elec.*, **Vol. 2**, 55–76, 1996.
- ⁴ Y. Suzuki, S. Sekine, and H. Toba, "A 1.3 micrometers optical transceiver diode module using passive alignment technique on a Si bench with a V-groove," *IEICE Trans. Electron.*, **Vol. 81**, 1508–1511, 1998.
- ⁵ M. Herrscher, M. Grundmann, E. Droge, S. Kollakowski, E. H. Botcher, and D. Bimberg, "Epitaxial liftoff InGaAs/InP MSM photodetectors on Si," *Electron. Lett.*, **Vol. 31**, 1383–1386, 1995.
- ⁶ M. S. Ünlü and S. Strite, "Resonant cavity enhanced photonic devices," *Appl. Phys. Rev.*, **Vol. 78** (2), 607–639, 1995.
- ⁷ M. K. Emsley, O. Dosunmu, and M. S. Ünlü, "Silicon Substrates with Buried Distributed Bragg Reflectors for Resonant Cavity-Enhanced Optoelectronics," *IEEE J. Select. Top. Quantum Elec.*, **Vol. 8** (4), 948–955, 2002.
- ⁸ M. Bruel, "Silicon on insulator material technology," *Elec. Lett.*, **Vol. 31** (14), 1201–1202, 1995.
- ⁹ K. Wada, H. Aga, K. Mitani, T. Abe, M. Suezawa, and L. C. Kimerling, "A New Approach of Photonic Bandgap Formation – Wafer Bonding and Delamination Technique," *International Conference on Solid State Devices and Materials*, **Vol. 30**, 382–383, 1998.
- ¹⁰ H.C. Luan, D. R. Lim, K. K. Lee, K. M. Chen, J. G. Sandland, K. Wada, and L. C. Kimerling, "High-quality Ge epilayers on Si with low threading-dislocation densities," *Appl. Phys. Lett.*, **Vol. 75** (19), 2909–2911, 1999.
- ¹¹ Y. Ishikawa, K. Wada, D. D. Cannon, Jifeng Liu, Hsin-Chiao Luan, and L. C. Kimerling, "Strain-induced band gap shrinkage in Ge grown on Si substrate," *Appl. Phys. Lett.*, **Vol. 82** (13), 2044–2046, 2003.
- ¹² W. C. Dash and R. Newman, "Intrinsic Optical Absorption in Single-Crystal Germanium and Silicon at 77°K and 300°K," *Phys. Rev.*, **Vol. 99** (4), 1151–1155, 1955.